

## X-ray photoelectron spectroscopy characterization of self-assembled monolayers for micromechanical biosensing applications

A.G. Mendoza-Madrigal \*

*Facultad de Nutrición, Universidad Autónoma del Estado de Morelos  
Cuernavaca, Mor. 62350 México*

A.J. Giménez, J.H. Mata Salazar <sup>β</sup>, G. Luna-Bárceñas, R. Ramírez-Bon, F.J. Espinoza-Beltrán  
*Centro de Investigación y de Estudios Avanzados del Instituto Politécnico Nacional, Unidad Querétaro.  
Santiago de Querétaro, Qro.76230 México*

<sup>β</sup> *Centro Nacional de Metrología  
Santiago de Querétaro, Qro.76246 México*

J.V. Méndez-Méndez

*Centro de Nanociencias y Micro y Nanotecnologías del Instituto Politécnico Nacional.  
Gustavo A. Madero, Cd. Méx. 07738 México*

(Received: April 29th, 2016; Accepted: September 5th, 2016)

Among the possible alternatives to microbiological techniques, small and extremely sensitive sensors called micromechanical oscillators are increasingly being used for the detection of very small masses or for stress sensing. Several types of biological bodies can be detected using micromechanical oscillators including proteins, peptides, viruses and bacteria. Therefore it is of great importance for the advancement of these detection methods to have a better understanding of the mechanisms used to attach the targeted bodies to the mechanical oscillators. In the present study, a silane-based self-assembled monolayers (SAM) are created over commercial cantilever mechanical oscillators. The fabricated SAMs are thoroughly characterized using high resolution angle-resolved XPS. A proof-of-concept experiment is conducted to study the performance of the characterized SAMs; this experiment is prepared in order to detect the interaction of the micromechanical oscillators with a protein (BSA) using a fluid cell from a BioAFM.

### Introduction

A biosensor is a device that measures physical and chemical variations going through over a biologically selective layer attached to a transducer when this layer interacts with a target molecule [1-4]. Most of the so called biosensors are built from gold, silicon, silicon nitride among other materials [5]. The used surfaces need to be functionalized with organic compounds, functionalization is done in order to attach and create a self-assembled monolayer that can interact specifically with a target molecule [6, 7]. As a potential replacement technology to normally implemented microbiological techniques, there have been proposed small sized, extremely selective, sensitive and fast-performing devices called micromechanical sensors, these sensors are increasingly being implemented to detect molecules by either mass variation or nanostress bending[8].

Micromechanical bending cantilevers have been used like biological and chemical sensors; the main advantage of these sensing methods is that the detection analyte requires no labelling and the various application fields only differ in the functional layers on the cantilever interface [9]. Atomic force microscopy (AFM) provides a convenient approach to create and evaluate microbiosensors; the use of cantilevers as force sensors in AFM is a sensing platform which offers excellent sensitivity and low detection limit [1, 10]. Cantilevers are of

particular interest because are easy to fabricate, can perform rapid real-time measurements and can be miniaturized for incorporation into lab-on-a-chip applications [11].

AFM has been used to measure the specific binding of individual ligand-receptor complexes or microorganism growth, this implies attaching specific biomolecules or chemical compounds onto AFM cantilevers [12]. Cantilevers can be operated in two basic modes, deflection (static) and resonant frequency measurements (dynamic); the first operation mode consists on the measurement of the differential stress when the target molecule interacts with the functionalized surface and the dynamic mode occurs when the molecular recognition take place producing a frequency shift due to aggregated mass on the functionalized surface[13].

A variety of techniques has been used to functionalize gold cantilever surfaces for biosensing [14]. A proposed strategy to functionalize gold surfaces for biosensor application would be: (Step 1) disable nonspecific adsorption of interference molecules; (Step 2) allow good accessibility to sensing molecules for kinetic measurements; (Step 3) provide the flexibility to substitute a variety of functional groups for immobilizing a wide range of sensing biomolecules; and (Step 4) retain the biological activity of the immobilized biomolecules.

Surface functionalization is used to modify the chemistry from the base material in order to make a linkage with

\* [gabriela.mendoza@uaem.mx](mailto:gabriela.mendoza@uaem.mx)

organic or biologic molecules [15, 16]. One of the most widely used methods for making a surface biocompatible is to treat the surface with silane coupling agents which act as intermediaries for the linkage with organic molecules that could be from bacteria, protein, phages, among other biomolecules.

Albumins are proteins of relatively small size (approximately 67 kDa) that constitute about 60 % of the protein mass found in blood plasma, they have a variety of physiological functions including; blood pressure regulation, transport of many small molecules in the blood such as bilirubin, calcium, progesterone [14,17]. It is important to notice that as albumin is the most abundant protein in the blood (near 40 mg/mL), it is expected that any implant materials will be exposed to albumin as soon as they are biologically inserted. From the reasons previously explained, it is of great importance to develop techniques for the proper characterization of protein sensing surfaces in micromechanical biosensing approaches.

The amount of protein adsorbed onto surfaces can be quantified by ellipsometry, quartz crystal microbalance, surface plasmon resonance, among other techniques. Another powerful technique is XPS which can be used to quantify and characterize the attachment of a self-assembled monolayer. X-ray photoelectron spectroscopy (XPS) is a very useful technique for the analysis of surfaces due to its capacity to measure the binding energy of only the outmost superficial atoms over the studied surface. From the information acquired it can be identified the presence of functional groups and chemical states over a surface. Using Angle Resolved XPS (ARXPS), it can be obtained information about elemental enrichment at the surface and a more detailed near-surface layer structure [18].

In the present work, we coupled a self-assembled [3-(2-aminoethylamino)propyl]trimethoxysilane monolayer on a micromechanical AFM cantilevers to achieve a functional surface to detect Bovine Serum Albumin (BSA) in a BioAFM using fluid cell. A deep characterization process has been proposed for the study of the obtained monolayers; from this characterization process it is expected to obtain both a better comprehension on the fabrication and operation of micromechanical biosensors.

## Materials and methods

### *Biosensor preparation (cleaning procedure)*

Triangular silicon nitride cantilevers coated with a  $45 \pm 5$  nm gold layer, having a nominal length of 205  $\mu\text{m}$  and a nominal spring constant of 0.06 N/m were used (DNP-S10, Bruker, Santa Barbara, CA). Cantilevers were washed sequentially in acetone, isopropyl alcohol, ethanol and water for 5 min each, to clean the surface prior to functionalization.

### *Self-Assembled Monolayers (film formation)*

Silane solution (0.1 M) was prepared in toluene. Fresh solutions were prepared the same day of the experiment since silanes are reactive to moisture.

The dissolved air was removed by degassing in a desiccator at aspirator vacuum for 30 min. Clean cantilevers were

placed at the top of a Petri dish and toluene dissolved [3-(2-aminoethylamino)propyl]trimethoxysilane was used to create a self-assembled monolayer. The solution was used to functionalize the gold surface by immersion overnight; the cantilevers were incubated inside a desiccator. After the silanization, the cantilevers were rinsed and dried under argon and maintained in a desiccator until its use [19].

### *Surface Analysis by XPS and FTIR*

For XPS and FTIR characterization analyses gold films evaporated over n-type phosphor-doped (100) silicon wafers were used. Over these gold surfaces was applied the same functionalization procedures performed over the cantilever devices in order to be able to study the surface chemistry.

XPS was used to quantify and characterize the attachment of the silane molecules onto a gold surface. XPS data were acquired using an Alpha 110 instrument of Thermo Electron (East Grinstead, UK) equipped with a monochromatic Al- $K_{\alpha 1}$  source, photon energy of 1486.7 eV and a seven-channel hemispherical detector, assembled by Intercovamex with a pass energy of 15 eV [20]. The binding energy (BE) scales for the monolayers on gold were referenced by setting the Au 4f<sub>7/2</sub> BE to 84.0 eV. The peak fitting was performed using AAnalyzer ® [21] with a Voigt line shape and a simultaneous fitting [22] for all the angles. An initial compositional survey scan was acquired, followed by high resolution spectra (N, C, O, Si, Au). Angle-resolved data were acquired at photoelectron takeoff angles of 35°, 45°, 65° and 85°, where the takeoff angle is defined as the angle between the sample surface and the axis of the spectrometer.

Atomic compositions were calculated from detailed spectra: C 1s (281 - 291 eV), O 1s (529 - 537 eV), N 1s (394 - 406 eV). The number of scans taken at different angles was adjusted to optimize the signal-to-noise ratio.

Transmission Fourier transform infrared (FTIR) vibrational spectroscopy was used to examine the proper functionalization of the cantilever surface with the [3-(2-aminoethylamino)propyl]trimethoxysilane. FTIR measurements in transmission mode were performed using a Perkin Elmer Spectrum GX operated with the Spectrum TM software v 5.3.1. Spectra were obtained within the range of 4000 - 400  $\text{cm}^{-1}$  by accumulating 24 scans at a spectral resolution of 4  $\text{cm}^{-1}$ .

### *Determination of the cantilever deflection*

The AFM setup consists of a fluid cell which is flushed by different solutions (PBS and BSA) through the injection system [23]. The functionalized cantilevers were placed in a 2.0 mg ml<sup>-1</sup> solution of Bovine serum albumin (BSA) that was prepared from lyophilized powder (Sigma Aldrich A763059, molecular weight ~ 66 kDa). The chamber is equipped with input and output tubes for flushing the solutions. The AFM detection system measures the deflection of the cantilever. The laser beam is focused on the cantilever; its reflection is collected by a photodetector allowing the calculation of the deflection [24].

For the biodetection experiments, an AFM (Bioscope Catalyst, Bruker) was used in static mode. The treated cantilever was immediately introduced into the analysis

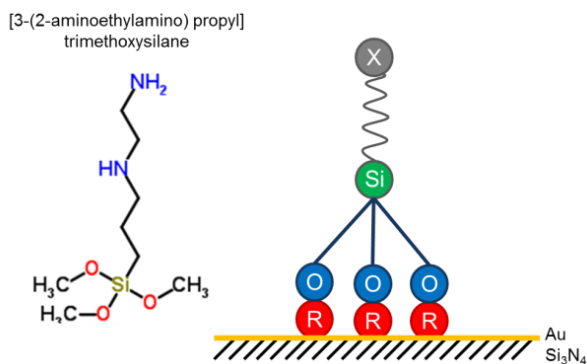


**Figure 1.** [3-(2-aminoethylamino)propyl]trimethoxysilane molecule, and the functionalization of a gold surface using. Image from RSC ChemSpider.

chamber using a fluid cell to measure the deflection (nm) of the cantilever when a solution of BSA dissolved in Phosphate Buffered Saline (PBS) was passed through it [25].

#### Optical characterization of the cantilever

An Optical Microscope (Contour GT-K 3D, Bruker) was used to characterize the surface of the cantilever after exposure to BSA in a fluid cell of an AFM.

### Results and discussion

FTIR and ARXPS were used in combination to understand the composition of the self-assembled monolayer and to evidence the proper functionalization prior to the biodetection experiments.

Figure 1 shows two different schematics of the [3-(2-aminoethylamino)propyl]trimethoxysilane molecule, which contains two functional groups; the inorganic group from the molecule interacts with the gold surface and the amine group interacts with the organic molecule (BSA). The silane molecules contain two types of reactive functional groups that are expected that are expected to appear in the FTIR spectrum [26]. FTIR spectroscopy is sensitive to surface molecular structure and can resolve closely spaced vibrational features.

To verify the surface functionalization, FTIR spectra were collected before and after the surface modification with [3-(2-aminoethylamino)propyl]trimethoxysilane. In the infrared spectra (Figure 2) some functional groups and classes of compounds are shown. The blue line corresponds to a silicon wafer and the green line corresponds to a silicon wafer with a gold coating, functionalized with [3-(2-aminoethylamino)propyl]trimethoxysilane.

As evidence of the proper functionalization of the studied surface, is the presence of the following bands: 1570  $\text{cm}^{-1}$  that corresponds to a primary amide (Figure 1) from the silane compound, peak shown in 1473  $\text{cm}^{-1}$  corresponds to a  $\text{CH}_2$  deformation, the band shown in 1318  $\text{cm}^{-1}$ , correspond to Si-C stretch (Figure 1). The previously mentioned bands are only present on the silane treated surface, on the non-treated surface is found a band related to Si-O-C stretch at 1106  $\text{cm}^{-1}$ ; this band is probably due to environment carbon present at the silicon wafer surface. Finally the band observed at 610  $\text{cm}^{-1}$  in both spectra corresponds to the base

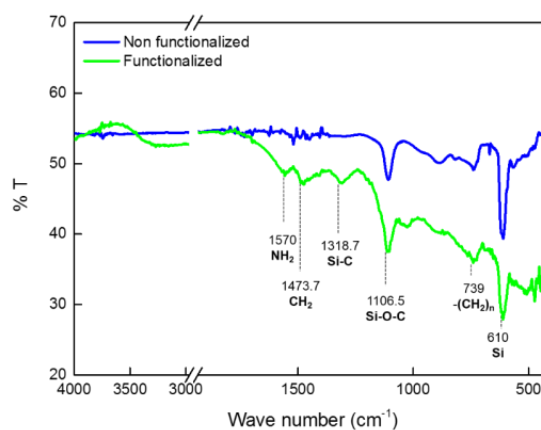


**Figure 2.** FTIR spectra of non-functionalized and silane functionalized surfaces.

material (silicon).

On the other hand, XPS can provide information about elemental distributions, layer or coating structure and thickness, as well as surface functionality evidence. XPS spectra probing the surface composition were taken after the surface functionalization. In Figure 3 the survey spectrum of [3-(2-aminoethylamino)propyl]trimethoxysilane functionalized surface, shows peaks from O, N, C, Si and Au, which is in agreement with the FTIR results that confirm the attachment of an organic film on the gold surface.

Figure 4 shows the high resolution XPS signals obtained from the C, O and N peaks; these signals have been deconvoluted in order to obtain their components. In figure 4(A), it can be observed C 1s measured peak and its components at: 286.2 eV (pink line) and 287.2 eV (green line), that might correspond to C-C, C-O, respectively; the blue line is associated with a C-N bond according to the atomic composition [14]. In Figure 4(B), O 1s measured peak and its components at: 533.3 eV (pink line), and 533.8 eV (green line) might correspond to C-O and Si-O, respectively; 535 eV (blue line) is associated with adventitious oxygen. In Figure 4(C), it can be observed N 1s measured peak and its components at: 400.4 eV (pink line) which corresponds to C-N and a peak at 401.8 eV (green line) which may be a C-N-C shift.

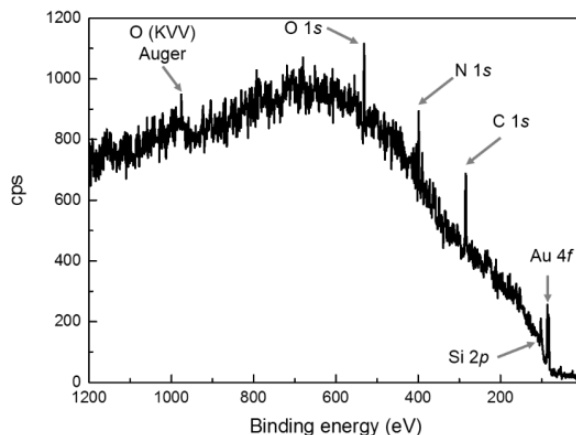


**Figure 3.** XPS survey spectra of a functionalized gold surface with [3-(2-aminoethylamino)propyl]trimethoxysilane.

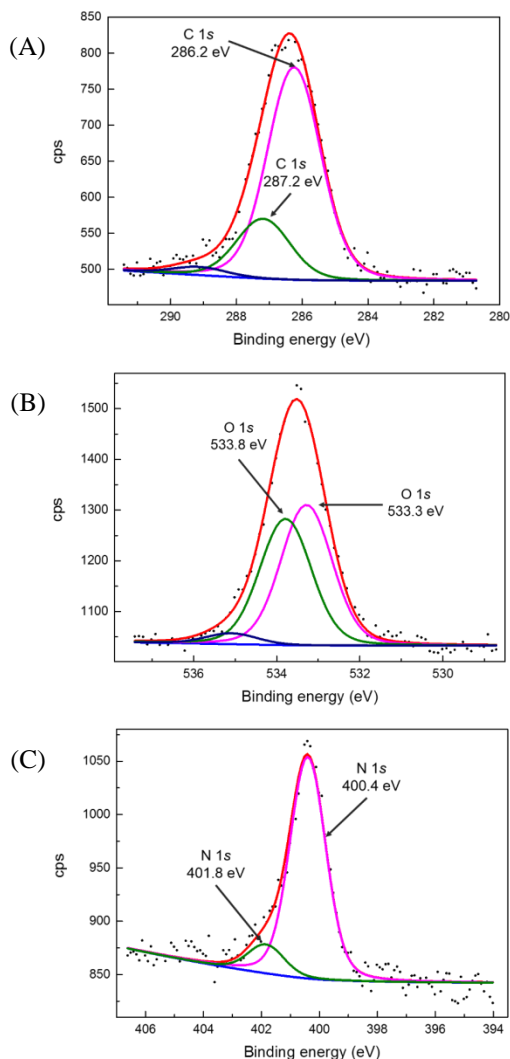


**Figure 4.** High resolution XPS measurements obtained for: (A) C 1s, (B) O 1s and (C) N 1s. Deconvoluted peaks are represented in curves of different colors.

In order to determinate the layer composition, Eq. (1) was used. This equation corresponds to a multilayer model; it is related to the intensity of the XPS signal emitted by the layer structure (Figure 1).

$$I_{i,q}(\alpha) = CA_i \lambda_{i,q} \rho_q \sin \alpha \left( 1 - \exp\left(-\frac{d_q}{\lambda_{i,q} \sin \alpha}\right) \right) \prod_{r=1}^{layers \text{ over } layer q} \exp\left(-\frac{d_r}{\lambda_{i,r} \sin \alpha}\right) \quad (1)$$

Where,  $I_{i,q}$  is the peak intensity of the  $i$  element placed at the  $q$  layer;  $\alpha$  is the angle between the spectrometer axis and the surface sample;  $A_i$  is the efficiency of the spectrometer at the peak energy  $i$  ( $A_i = 1/KE_i$ , where  $KE_i$  is the kinetic energy of the electrons);  $\lambda_{i,q}$  is the Electron Effective Attenuation Length (EAL) of the electrons of the peak  $i$  passing through

**Table 1.** Atomic composition of the self-assembled monolayer.

Peaks	Binding energy (eV)	Proportion (%)
C 1s	284.4	58
O 1s	531.5	19
N 1s	398.3	12
Si 2p	101.1	11

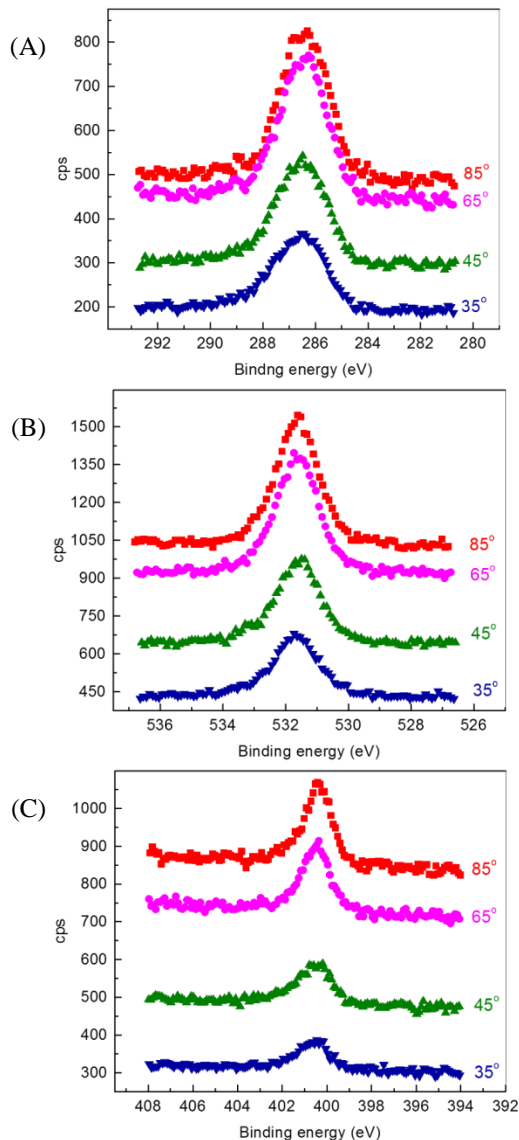


**Figure 5.** High resolution angular XPS peaks for (A) C, (B) O and (C) N.

the  $q$  layer;  $d_q$  is the thickness of the  $q$  layer, and  $C$  is a constant independent from the element or angle [27]. This equation was used to determine the composition and the thickness  $d_q$  of the self-assembled monolayer. The ARXPS data used to perform these calculations is shown in Figure 5 for (A) C, (B) O and (C) N. A graphic representation of the SAM is depicted in Figure 6.

The composition results are shown in Table 1; the intensity of the C 1s peak is assigned the value 1 and the other elements are normalized by their intensity.

The cantilever deflection produced by the attached protein was measured. PBS (control) or BSA solution (target analyte) was flushed in the fluid cell during 30 min. Figure 7 shows the results of the biodetection experiments for the cantilever deflection in the presence of PBS and BSA during 30 min. In the control experiment (functionalized cantilever+PBS) there was no detected deflection during this period of time. On the other hand, with the functionalized cantilever+BSA, immediately after the BSA injection, there is a 3-minutes

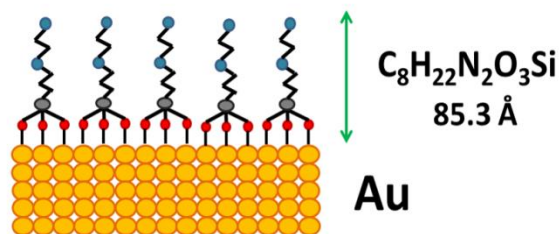


**Figure 6.** Representation on the self-assembled monolayer of [3-(2-aminoethylamino)propyl]trimethoxysilane over gold surface. The thickness data calculated from ARXPS analysis (Eq. 1) is 85.3 Å.

stabilization period and then the cantilever deflection starts to increase linearly during the exposure to BSA solution. After 20 min, the total shift was about 2.5 nm indicating that the BSA was attached to the functionalized cantilever. After 22 min of biodetection experiments, a stationary phase can be seen, probably due to the available site depletion caused by protein interaction.

In Figure 8(A) the surface of a cantilever after cleaning procedure can be seen where a smooth, clean and particle free surface is observed. Figure 8(B) shows the same cantilever after 30 min of biodetection experiment which consisted on a fluid cell that flushed a BSA solution containing the target molecule; the identified changes on the surface are due to the biodetection over the previously functionalized surface; because of the strong interactions, the protein molecules lose their native conformation upon adsorption and are highly aggregated forming a tightly bound and highly entangled polypeptide film.

## Conclusions

Self-assembled monolayers built over micromechanical cantilever devices, have been thoroughly characterized principally using high resolution angle resolved XPS. Analyzing the results obtained from the XPS measurements, the detailed composition of the formed monolayers is calculated. In this work this type of analysis is demonstrated to be a valuable tool to study the characteristic of SAMs to be implemented for biosensing applications. FTIR is used in order to corroborate the presence of an organic layer over the functionalized surface. To demonstrate the proper operation

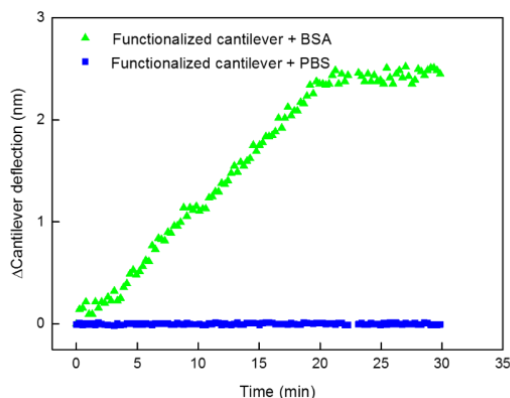


**Figure 7.** Data trace for control experiments and after exposure to BSA in fluid cell.

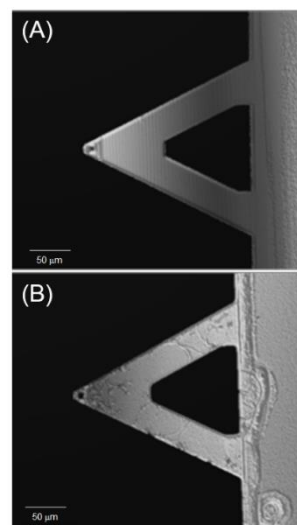


**Figure 8.** Optical images of (A) bare DNP-S10 cantilever and (B) functionalized cantilever, after 30 min of biodetection experiments in an AFM fluid cell.

of the obtained SAMs, a proof-of-concept experiment was performed in order to detect BSA protein. From optical microscopy observations, it can be seen that the change on the cantilever surface was due to the interactions of the functionalized area and the BSA (target analyte), which generated a bending stress over the cantilever that was measured by the deflection (nm) detected using AFM. In order to measure real time detection of BSA a BioAFM cell has been implemented where the bio sensing cantilevers are exposed to both a BSA containing solution and a buffer control solution. Experiments done using control solution do not show any cantilever deflection, at the other hand when applying a BSA containing solution there is an immediate response stabilizing 30 minutes later from the initial exposure. The characterization methods applied in this work could be used as a valuable reference for the further development of biosensors for applications in the medical, pharmaceutical, environmental or food industry.

## Acknowledgments

This work was supported by CONACYT from Mexico. The authors want to acknowledge Reina Araceli Mauricio Sanchez, Carlos Alberto Ávila Herrera, Alfredo Muñoz Salas and Gustavo Gómez Sosa for their technical support and Barbara Hacker from Peace Corps for the proof reading. CONACyT (Dr. Espinoza) MEZFER-213108 (Dr. Luna).

## References

- [1]. V. Velusamy, K. Arshak, O. Korostynska, K. Oliwa, C. Adley, *Biotechnol. Adv.* **28**, 232 (2010).
- [2]. R. van den Hurk, S. Evoy, *Sensor. Actuat. B-Chem.* **176**, 960 (2013).
- [3]. N. Nugaeva, K.Y. Gfeller, N. Backmann, H.P. Lang, M. Duggelin, M. Hegner, *Biosensors Bioelectron.* **21**, 849 (2005).
- [4]. U. Sungkanak, A. Sappat, A. Wisitorsaat, C. Promptmas, A. Tuantranont, *Biosensors Bioelectron.* **26**, 784 (2010).
- [5]. J. Tamayo, P.M. Kosaka, J.J. Ruz, A. San Paulo, M. Calleja, *Chem. Soc. Rev.* **42**, 1287 (2013).
- [6]. A.G. Mendoza Madrigal, J.J. Chanona Pérez, H. Hernández

- Sánchez, E. Palacios González, G. Calderon Domínguez, J.V. Mendez Mendez, J. Blasco, L.A. Villa Vargas, *Rev. Mex. Ing. Quím.* **12**, 205 (2013).
- [7]. H. Joung, W. Shim, D. Chung, J. Ahn, B. Chung, H. Choi, S. Ha, K. Kim, K. Lee, C. Kim, K. Kim, M. Kim, *Biotechnol. Bioproc. Eng.* **12**, 80 (2007).
- [8]. B. Ilic, D. Czaplewski, M. Zalalutdinov, H.G. Craighead, P. Neuzil, C. Campagnolo, C. Batt, *J. Vac. Sci. Technol. B*, **19**, 2825 (2001).
- [9]. A. Berquand, N. Xia, D.G. Castner, B.H. Clare, N.L. Abbott, V. Dupres, Y. Adriaensen, Y.F. Dufrane, *Langmuir* **21**, 5517 (2005).
- [10]. M. Alvarez, L.M. Lechuga, *Analyst* **135**, 827 (2010).
- [11]. P.S. Waggoner, H.G. Craighead, *Lab Chip* **7**, 1238 (2007).
- [12]. R. Raiteri, M. Grattarola, H.-J. Butt, P. Skladal, *Sensor. Actuat. B-Chem.* **79**, 115 (2001).
- [13]. B. Dhayal, W.A. Henne, D.D. Doorneweerd, R.G. Reifenger, P.S. Low, *J. Am. Chem. Soc.* **128**, 3716 (2006).
- [14]. H.B. Lu, C.T. Campbell, D.G. Castner, *Langmuir* **16**, 1711 (2000).
- [15]. B. Lee, T. Nagamune, *Biotechnol. Bioproc. Eng.* **9**, 69 (2004).
- [16]. J. Choi, J. An, B. Kim, *Biotechnol. Bioproc. Eng.* **14**, 6 (2009).
- [17]. B. Fang, Q. Ling, W. Zhao, Y. Ma, P. Bai, Q. Wei, H. Li, C. Zhao, *J. Membrane Sci.* **329**, 46 (2009).
- [18]. D.R. Baer, M.H. Engelhard, *J. Electron. Spectrosc. Relat. Phenom.* **178**, 415 (2010).
- [19]. A. Ebner, P. Hinterdorfer, H.J. Gruber, *Ultramicroscopy*, **107**, 922 (2007).
- [20]. A. Herrera-Gomez, M. Bravo-Sanchez, F.S. Aguirre-Tostado, M.O. Vazquez-Lepe, *J. Electron. Spectrosc. Relat. Phenom.* **189**, 76 (2013).
- [21]. "The peak-fitting software employed was AAnalyzer® ([www.rdata.com.mx/AAnalyzer](http://www.rdata.com.mx/AAnalyzer))".
- [22]. J. Muñoz-Flores, A. Herrera-Gomez, *J. Electron. Spectrosc. Relat. Phenom.* **184**, 533 (2012).
- [23]. H.P. Lang, M. Hegner, C. Gerber, *Mater. Today* **8**, 30 (2005).
- [24]. F.J.E. Beltrán, J. Muñoz-Saldaña, D. Torres-Torres, R. Torres-Martínez, G.A. Schneider, *J. Mater. Res.* **21**, 3072 (2006).
- [25]. G. Longo, L. Alonso Sarduy, L.M. Rio, A. Bizzini, A. Trampuz, J. Notz, G. Dietler, S. Kasas, *Nat. Nanotechnol.* **8**, 522 (2013).
- [26]. N. Kohler, G.E. Fryxell, M. Zhang, *J. Am. Chem. Soc.* **126**, 7206 (2004).
- [27]. M.P. Seah, J.H. Qiu, P.J. Cumpson, J.E. Castle, *Surf. Interface Anal.* **21**, 336 (1994).